Journal of Ethnopharmacology 165 (2015) 94–102

Contents lists available at ScienceDirect

Journal of Ethnopharmacology

journal homepage: www.elsevier.com/locate/jep

Research Paper

Bioassay-guided isolation and mechanistic action of anti-inflammatory agents from *Clerodendrum inerme* leaves

Klaokwan Srisook [a,b,*], Ekaruth Srisook [b,c,**], Wenuka Nachaiyo [a], Mingkwan Chan-In [a], Jitra Thongbai [a], Karnjanapa Wongyoo [a], Sasithorn Chawsuanthong [a], Kanita Wannasri [a], Sudarat Intasuwan [a], Kingkan Watcharanawee [a]

[a] Department of Biochemistry, Faculty of Science, Burapha University, Muang, Chonburi 20131, Thailand
[b] Centre of Excellence for Innovation in Chemistry, Burapha University, Muang, Chonburi 20131, Thailand
[c] Department of Chemistry, Faculty of Science, Burapha University, Muang, Chonburi 20131, Thailand

ARTICLE INFO

Article history:
Received 3 November 2014
Received in revised form
16 February 2015
Accepted 17 February 2015
Available online 26 February 2015

Chemical compounds studied in this article:
Acacetin (PubChem CID: 5280442)
Hispidulin (PubChem CID: 5281628)
Diosmetin (PubChem CID: 5281612)

Keywords:
Clerodendrum inerme
Nitric oxide
Prostaglandin E_2
Anti-inflammatory
Flavone

ABSTRACT

Ethnopharmacological relevance: The leaves of *Clerodendrum inerme* (L.) Gaertn. have commonly been used in Thai traditional medicine for treatment of inflammatory diseases. However, the bioactive compounds responsible for the anti-inflammatory effect of leaves have not been yet determined. The objective of the present study was to isolate these bioactive compounds by bioassay-guided isolation technique and to determine the mode of action of isolated compounds in LPS-induced macrophages.
Materials and methods: Anti-inflammatory effect of various fractions (hexane, ethyl acetate and water) of ethanol extract of *C. inerme* leaves was determined from the production of nitric oxide (NO) in RAW 264.7 macrophage stimulated with LPS. The mRNA and protein levels were determined also by real-time reverse transcription-polymerase chain reaction and western blot analysis, respectively. Leaf bioactive compounds were isolated by bioassay-guided fractionation technique using column chromatography.
Results: The ethyl acetate fraction (EA) among solvent extracts provided the most potent inhibitory activity on NO production. Also, EA reduced the mRNA and protein expressions of inducible nitric oxide synthase (iNOS) in LPS-stimulated macrophages. Three known flavones, acacetin (**1**), hispidulin (**2**) and diosmetin (**3**), were isolated based on inhibition of NO production. Furthermore, hispidulin also inhibited PGE_2 production as well as iNOS and cyclooxygenase-2 expressions via the blockade of NF-κB DNA-binding activity and JNKway.
Conclusions: Our results found acacetin (**1**), hispidulin (**2**) and diosmetin (**3**), were responsible for the anti-inflammatory properties of *C. inerme* leaves. We provide scientific evidence to support the usefulness of *C. inerme* leaves in traditional medicine for the treatment of inflammation-related diseases.

1. Introduction

Inflammation is a response of the body to harmful stimuli such as injury and infection (Kumar et al., 2007). Macrophages are principally involved in acute and chronic inflammation. Upon activation, they secrete a series of pro-inflammatory mediators including nitric oxide (NO), prostaglandin E_2 (PGE_2), tumor necrosis factor-α (TNF-α) and interleukin-1β (IL-1β). An overproduction of these mediators causes a harmful effect to tissues and organisms as well as has been associated with the pathogenesis of various inflammatory-related diseases, including rheumatoid arthritis, diabetes, inflammatory bowel disease, atherosclerosis, and cancer (Yang et al., 2013).

Clerodendrum inerme (L.) Gaertn. (Verbenaceae family) known also as Sam-Ma-Nga in Thai or, seaside *clerodendrum* in English, occurs widely in coastal mangrove forests of Thailand (Office of Mangrove Resources Conservation, 2009) and other South Asian countries and is used in traditional medicine for the treatment of skin diseases, rheumatic pain and arthritis, fever, cough, hepatitis, and other inflammatory diseases (Shrivastava and Patel, 2007a; Chethana et al., 2013). The major chemical constituents of *C. inerme* are flavonoids, terpenes, steroids and phenolic compounds (Shrivastava and Patel, 2007b; Parveen et al., 2010; Shahabuddin et al., 2013). *C. inerme* possesses a number of biological activities including antimicrobial, anti-hepatotoxic, anti-oxidant, analgesic and anti-inflammatory activities (Gopal

* Corresponding author at: Department of Biochemistry, Faculty of Science, Burapha University, Chonburi 20131, Thailand.
Tel.: +66 38 103 058Ext12; fax: +66 38 393 495.
** Corresponding author at: Department of Chemistry, Faculty of Science, Burapha University, Chonburi 20131, Thailand.
Tel.: +66 38 103 009; fax: +66 38 745 789.
E-mail addresses: klaokwan@buu.ac.th (K. Srisook), ekaruth@buu.ac.th (E. Srisook).

http://dx.doi.org/10.1016/j.jep.2015.02.043
0378-8741/

and Sengottuvelu, 2008; Gurudeeban et al., 2010; Yankanchi and Koli, 2010; Sangeetha et al., 2011; Chethana et al., 2013). Methanol extract of *C. inerme* leaves is reported to inhibit sub-chronic inflammation in cotton pellet-induced granuloma in mice (Yankanchi and Koli, 2010). Recently, ethanol extracts of *C. inerme* exhibited anti-inflammatory in carrageenan-induced paw edema and xylene-induced ear edema (Kalavathi and Sagayagiri, 2014; Khanam et al., 2014). Such in vivo anti-inflammatory activities of *C. inerme* indicated the presence of anti-inflammatory agents. However, the bioactive compounds responsible for the anti-inflammatory effect of *C. inerme* are not explored. To find out scientific evidence for therapeutic uses of *C. inerme* leaves, the objective of the present study was to identify the compounds responsible for the anti-inflammatory activity based on inhibition of NO production of *C. inerme* leaves through bioassay-guided isolation. We investigated the mechanism behind their anti-inflammatory activity on LPS-induced RAW 264.7 macrophages to assess the effectiveness of *C. inerme* leaves for various inflammatory diseases.

2. Material and methods

2.1. Reagents

Antibodies for p44/42 MAPK (ERK1/2), p38 MAPK and lamin A were bought from Santa Cruz Biotechnology (Santa Cruz, CA, U.S.A). Antibodies for phospho-p44/42 MAPK (ERK1/2) (Thr202/Tyr204), phospho-p38 MAP kinase (Thr180/Tyr182), SAPK/JNK, phospho-SAPK/JNK (Thr183/Tyr185), NF-κBp65 and goat anti-mouse IgG conjugated horseradish peroxidase secondary antibodies were purchased from Cell Signaling Technology (Danvers, MA, USA). Anti-mouse β-actin antibody, lipopolysaccharide or LPS (*Escherichia coli* serotype O111:B4), 3-(4, 5-dimethylthiazol-2-yl)-2,5-diphenyltetrazolium bromide (MTT), Dulbecco's modified Eagle's medium (DMEM) free of phenol red were all obtained from Sigma Chemical (St. Louis, MO, USA). DMEM, fetal bovine serum (FBS), penicillin–streptomycin were purchased from Invitrogen/Gibco (Grans Island, NY, USA). Antibodies for iNOS and COX-2 were obtained from BD Bioscience (San Jose, CA, USA.). iScript™ Reverse Transcription Supermix for RT-qPCR and iTaq™ Universal SYBR®Green Supermix were bought from BIO-RAD (Hercules, CA, USA). Oligonucleotide primers were obtained from Sigma-Aldrich (Singapore). PGE_2 enzyme immunoassay kit was bought from R&D Systems (Minneapolis, MN, USA.). Protease inhibitor cocktail tablets and Phosphatase inhibitor cocktail tablets (PhosStop) were purchased from Roche (Germany). Super Signal West Pico Chemiluminescent substrate was obtained from Pierce (Rockford, IL, USA). TRI reagent was bought from Molecular Research Center (Cincinnati, OH, USA). TransAm NF-κB kit was purchased from Active Motif (Tokyo, Japan). Silica gel 60, used for chromatographic technique, was purchased from Merck (Germany).

2.2. Plant material

C. inerme (L.) Gaertn. (The Plant List record 42703) was collected from Welu wetland, Chantaburi Province, Thailand, GPS coordinates: 12° 22′ 05.82″ N to12° 22′ 15.42″ N, 102° 20′ 26.35″ E to 102° 20′ 27.22″ E in May 2010. The plant was identified by Dr. B. Chewprecha, Department of Biology, Faculty of Science, Burapha University. A voucher specimen (KS-SCBUU-0016) is kept at Faculty of Science, Burapha University.

2.3. Plant extraction, isolation and elucidation

Leaves of *C. inerme* were washed in tap water, dried at 50 °C, and finally ground in a blender. Ground leaves (1.2 kg) were macerated in ethanol (12 L) at room temperature for 5 days with occasionally shaking and filtered through Whatman filter paper no. 3. The plant residue was then re-extracted with ethanol twice as described above. Filtrates were pooled and evaporated in vacuo. The ethanol extract (EE, 195 g,16.2% w/w) was then partitionally separated to yield the residues of hexane (HF, 36.7 g, 21.7% w/w), ethyl acetate (EF, 26.7 g, 15.8% w/w), and water (WF, 98.5 g, 58.3% w/w) fractions, respectively. Fractions were kept at −20 °C and protected from light until investigated for their anti-inflammatory effects.

Ethyl acetate fraction was chosen for further studies due to its high potent inhibitory effect on NO production in LPS-induced macrophages. The ethyl acetate fraction (EF, 17 g) was separated by column chromatography using silica gel as stationary phase. Solvent system (dichloromethane: methanol) gradient from 100:0 to 50:50 v/v was used to isolate subfraction 1–8 (F1–F8) from EF. Based on anti-inflammatory activity, the subfraction F5 (1.3549 g, 0.11% w/w) was then subjected to silica gel column with step gradient of ethyl acetate and hexane (30:70, 50:50 and 70:30 v/v) to obtain 8 subfractions (SF5.1–5.8). Based on anti-inflammatory activity, the subfraction SF5.1 and 5.2 were pooled (0.810 g, 0.07% w/w) and loaded on to silica gel column chromatography and eluted to obtain compound **1** (119 mg), **2** (129.7 mg) and **3** (6 mg).

Subfraction F8 (2.930 g, 0.24% w/w) was loaded onto a silica gel column and eluted with a gradient of dichloromethane: methanol (99:1–80:20, v/v) to obtain 4 subfractions (SF8.1–8.4). SF8.1 (0.1662 g, 0.01% w/w) was, based on its anti-inflammatory activity, further submitted to silica gel column using a gradient of dichloromethane: methanol (97:3–92:8, v/v) as the mobile phase obtaining compound **1** (4.1 mg). SF 8.2 (0.2648 g, 0.02% w/w) was consequently separated in a silica gel column with a gradient of hexane-ethyl acetate (70:30–95:5, v/v) to obtain compound **2** (12.6 mg). Yields of compound **1**, **2** and **3** were 0.0103%, 0.0118% and 0.0005%, respectively. The scheme showing fractionation procedure of *C. inerme* leaves is shown in Fig. 1.

Proton NMR and Carbon NMR spectra were recorded on a Bruker AVANC 400 at 400 and 100 MHz, respectively. All spectra were measured in $CDCl_3$, DMSO-d_6 and methanol-d_4 solvents and chemical shifts are reported as δ values in parts per million (ppm) relative to solvent peak as internal standard.

2.4. Cell culture

RAW 264.7 murine macrophage cell line was a gift from Prof. C. Kim, Inha University College of Medicine, Republic of Korea. Cells were cultured in DMEM containing 25 mM D-glucose, 100 U/mL of penicillin,100 μg/mL of streptomycin and 10% heat-inactivated FBS. Cells were incubated at 37 °C in 5% CO_2 atmosphere.

2.5. Cell viability test by MTT assay

RAW 264.7 macrophages were plated into a 24-well plate (1.5×10^5 cells/well). After an overnight growth, media containing various concentrations of the test compounds were added to wells for an indicated time. 10 μL of MTT solution (5 mg/mL in PBS) was put into each well for 2–3 h before aspiration of the solution. 500 μL of dimethyl sulfoxide (DMSO) was added into each well to solubilize the blue formazan crystal product. Subsequently, the formazan solution was measured the absorbance at 550 nm using a microplate reader (Molecular Device, USA.). The amount of formazan was proportional to the number of functional mitochondria in viable cells. Percentage of cell viability was expressed as: (absorbance of treated well/absorbance of control well) × 100.

2.6. Determination of nitrite and PGE_2 concentration

Nitrite is a stable oxidation product of NO, a major pro-inflammatory mediator involved in various inflammation-related

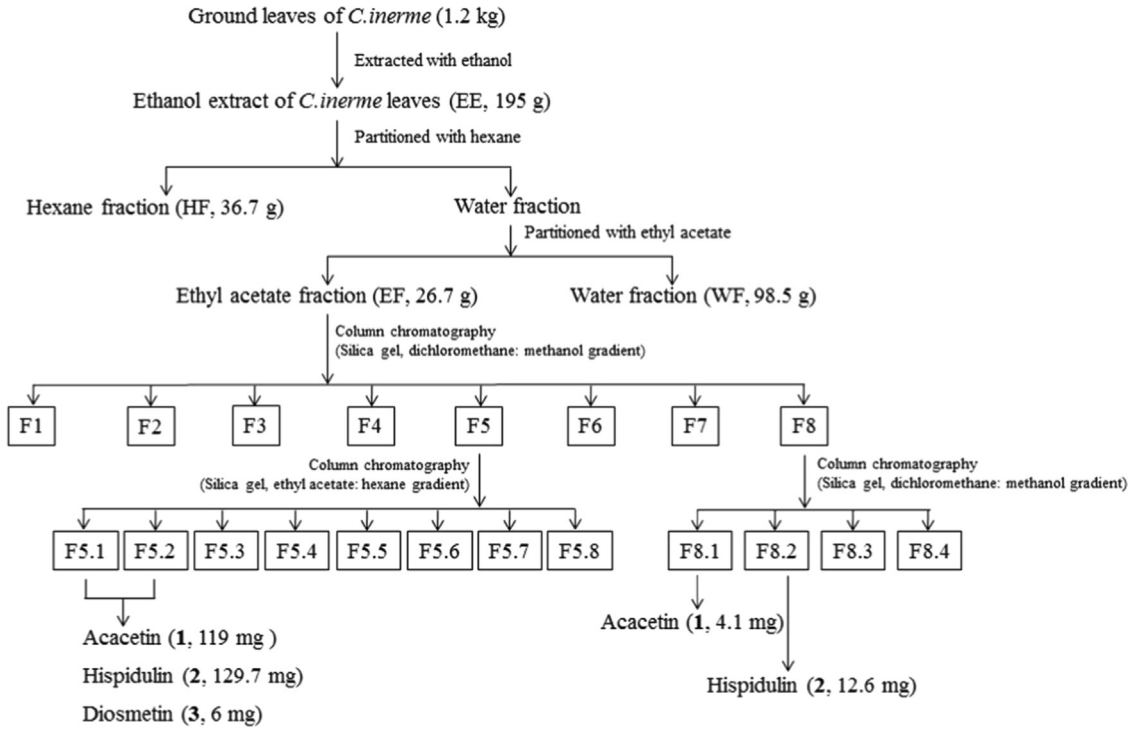

Fig. 1. Extraction and fractionation scheme of *C. inerme* leaves.

diseases. Nitrite present in condition media is used as an index of iNOS activity in LPS-stimulated macrophages. Cells were plated on a 24-well plate and treated with the test compounds for 24 h. Collected culture media (100 μL) were mixed with an equal volume of Griess reagent (0.1% N-(1-naphtyl)-ethylenediamine and 1% sulfanilamide in 5% orthophosphoric acid) and incubated at room temperature for 10 min. The formation of an azo compound was followed spectrophotometrically at 546 nm in a microplate reader. Nitrite concentration was determined from a standard curve of sodium nitrite made up in phenol red-free DMEM. PGE_2 present in culture media from LPS-activated RAW 264.7 cells was quantified using PGE_2 competitive enzyme immunoassay kit (R&D Systems, USA).

2.7. Western blot analyses for protein expression

RAW 264.7 cells (1×10^6 cells/60-mm plate) were plated and treated with tested compounds. After 24 h, cells were washed twice with ice-cold phosphate-buffered saline (PBS), pH 7.4 and scraped in the presence of cold RIPA lysis buffer [150 mM Tris–HCl (pH 7.4), 150 mM NaCl, 5 mM EGTA, 0.1% (w/v) SDS, 1% (w/v) sodium deoxycholate, and 1% (v/v) Nonidet P-40] containing 1 mM DL-1,4-dithiothreitol (DTT) and a mixture of protease inhibitors (Complete mini, Roche, Germany). Cell lysates were centrifuged at 12,000*g* for 10 min at 4 °C. Protein concentrations in the supernatant were determined with a BCA protein assay kit (Pierce, USA). Equal amounts of soluble protein were separated onto 10% SDS-polyacrylamide gel electrophoresis (SDS-PAGE) and transferred to a PVDF membrane. The non-specific bindings were blocked with 5% (w/v) non-fat dried milk solution dissolved in TBS-T buffer (10 mM Tris–HCl, pH 7.4, 100 mM NaCl and 1% (v/v) Tween 20) for 1 h at room temperature. The membrane was incubated with specific primary antibodies for an appropriate length of time, subsequently incubated with goat anti-mouse or goat anti-rabbit IgG conjugated with horseradish peroxidase secondary antibodies. After that, specific protein bands on PVDF membranes were detected on X-ray film activated with enhanced chemiluminescence using SuperSignal West Pico Chemiluminescent. Intensities of each band signal were determined by densitometry using BIOPROFIL Bio-1D version 11.9 (Villber Lourmat Biotechnology). Image densities of specific bands for iNOS and COX-2 were normalized with a density of β-actin band.

For determination of the level of phosphorylated MAPKs, cells were scraped in the presence of 100 μL of ice-cold RIPA lysis buffer containing 1 mM DTT, a mixture of phosphatase and protease inhibitors. Proteins in supernatant were subjected to electrophoresis using 10% SDS-PAGE and undertaken immunoblotting as described above. Image densities of specific bands for p-p38, p-JNK and p-ERK were normalized with the density of total p38, total JNK and total ERK band, respectively.

Nuclear translocation of NF-κB was determined from nuclear protein which extracted by the method of Buapool et al. (2013). Protein concentration was determined with a Quick Start Bradford protein assay kit (Bio-Rad, USA.) and followed by a Western blot analysis as described above. Image density of NF-κB p65 subunit band for nuclear protein was normalized with the density of lamin A band.

2.8. Real time reverse transcription-polymerase chain reaction (real time RT-PCR)

RAW 264.7 cells (1×10^6 cells/60-mm plate) were plated and treated with tested compounds. Total cellular RNA was isolated after 9 h with TRI reagent (Molecular Research Center, U.S.A.) according to the manufacturer's instruction. 1 μg of total RNA was reverse-transcribed to make cDNA using iScript™ Reverse Transcription Supermix for RT-qPCR (Bio-Rad, USA.). The reaction mixer contained 4 μL of 5 × supermix, total RNA and DNase-free water to make up volume to 20 μL and was incubated at 25 °C for 5 min, at 42 °C for 30 min and at 85 °C for 5 min. Complementary DNA (cDNA) was used in real-time RT-PCR. Quantitative real-time PCR was conducted on CFX96 Touch™ Real-Time PCR (Bio-rad, USA.). Specific primers for the iNOS, COX-2 and elongation factor-2 (EF-2) were as follows: iNOS, 5′-GCACAGCA-CAGGAAATGTT TCAGCAC-3′ (f) and 5′-AGCCAGC ATACCGGATGAGC-3′

(r) from accession number NM_010927.2; COX-2, 5′-TGATCGA AGACTACGTGCAACACC-3′ (f) and 5′-TTCAATGTTGAAGGTGTCGGGCAG-3′ (r) from accession number NM_011198.3; EF-2, 5′-CTGAAGCGGCTGGCTAAGTCTGA-3′ (f) and 5′-GGGTCAGATTTCTTGATGGGGAT-3′ from accession number NM_001961.3. The total 20 μL reaction mixture contained 10 μL of 2 × iTaq™ Universal SYBR®Green Supermix (Bio-rad, USA.), 250 nM of specific primer and 2 μL of cDNA. The PCR cycling parameters were set as follows: pre-heat at 95 °C for 3 min followed by 40 cycles of PCR reactions at 95 °C for 10 s and 63 °C for 20 s. The relative quantification of target mRNA was calculated from formula $2^{-\Delta\Delta CT}$ as described by Giulietti et al. (2001). EF-2 mRNA level (housekeeping gene) was used as internal control.

2.9. NF-κB DNA-binding assay

Cells (5×10^6 cells/100-mm plate) were incubated overnight for attachment, then exposed to hispidulin for 30 min prior to treatment with LPS for 1 h. Cells were washed twice with ice-cold PBS and nuclear protein was extracted using NE-PER nuclear and cytoplasmic extraction reagents (ThermoScientific, USA) according to the manufacturer's instructions. Protein concentration was determined with a BCA protein assay kit (Pierce, USA). The DNA binding activity of nuclear NF-κB p65 subunit was evaluated with a TransAM NF-κB p65 kit (Active Motif, Japan) which is an ELISA-based transcription factor assay kit according to the manufacturer's instructions. Activated NF-κB in nuclear protein extract binds to immobilized oligonucleotide containing NF-κB consensus site. The primary antibody specific to epitope of NF-κB p65 subunit is accessible to NF-κB subunit bound to its target DNA. An HRP-conjugated secondary antibody was then added to quantify the amount of activated NF-κB.

2.10. Statistical analysis

All experiments were replicated at least three times. Data are presented as mean ± SEM. One-way analysis of variance and two-tailed student's *t*-test was used to determine statistical significance. A *P* value of < 0.05 was considered statistically significant.

3. Results and discussion

The ethyl acetate fraction (EA) among plant extracts provided the most potent inhibitory activity on iNOS-catalyzed NO production in RAW 264.7 macrophages (Fig. 2A). Nitrite concentration increased significantly from 0.7 ± 0.1 μM in unstimulated cells to 36.9 ± 3.6 μM after treatment with LPS for 24 h. The inhibitory effect of EA on NO production in cells treated with LPS corresponding to 75.7 ± 4.2% at concentration of 50 μg/mL (Fig. 2A). Cell viability of LPS-treated macrophages was not altered by other extracts except HF (Fig. 2B). Actually, HF exhibited a slight decline in cell viability. These data suggested the NO inhibitory effect of the plant extracts was not due to their cytotoxicity. Based on the anti-inflammatory effect, EF was chosen for further studies. EF inhibited LPS-induced NO production in a dose-dependent manner with an IC_{50} value of 32.9 ± 3.9 μg/mL (Fig. 3A). A known iNOS inhibitor, aminoguanidine (Alderton, 2001) at 50 μM (6.8 μg/mL) inhibited NO production to 56.2 ± 2.7%. Also, it suppressed iNOS protein expression in a dose-dependent manner (Fig. 3B). EF alone did not affect iNOS protein expression when compared to unstimulated cell or DMSO-treated cells.

Nitric oxide production reflecting inhibitory activity was used to guide the isolation of compounds responsible for the anti-inflammatory effect of EF. Subfractions 1–8 (F1–F8) were obtained from fractionation of EF by silica gel column chromatography. Based on anti-inflammatory effects without cytotoxicity shown in Fig. 4A and B, subfractions SF5 and SF8 were further isolated. Subfractions 5.1 and 5.2 showing the high NO inhibitory activity

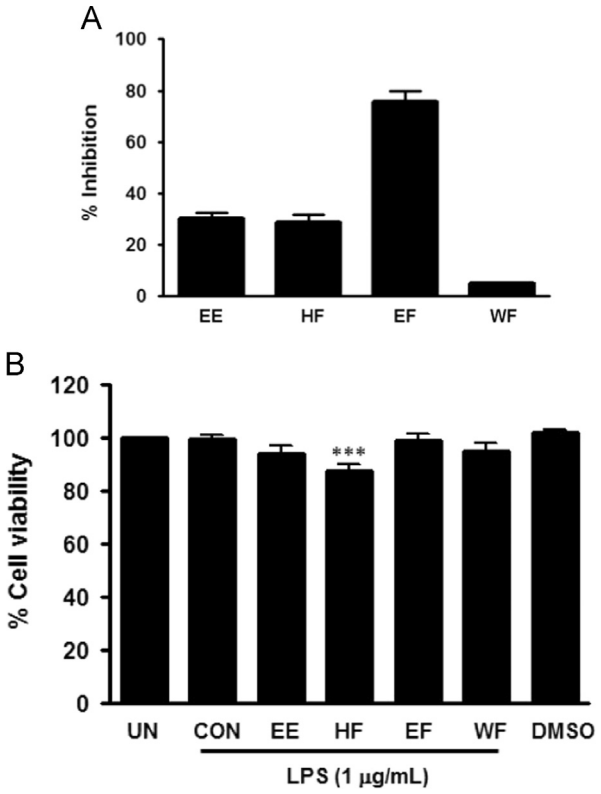

Fig. 2. Inhibitory activities of ethanol leaf extract of *C. inerme* and its fractions against NO production. Macrophages were incubated with LPS and the plant extracts for 24 h. (A) Nitrite concentration in cultured media were determined by Griess reaction. The percentage inhibition of NO production of each treatment was determined in comparison to LPS-stimulated RAW264.7 macrophage cells. (B) Cell viabilities were determined by MTT assay. Each column shows the mean ± SE of three independent experiments with triplicate samples. ***$p < 0.001$ vs unstimulated cells. UN=unstimulated control cells, CON=LPS-stimulated cells and DMSO=0.2% (v/v) DMSO-treated cells, EE= ethanol extract, HF=hexane fraction, EF=ethyl acetate fraction, WF=water fraction.

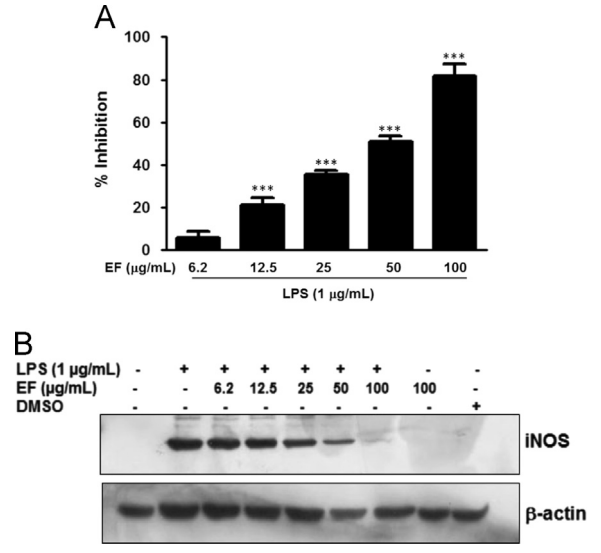

Fig. 3. Inhibitory effect of EFon NO (A) and iNOS expression (B) in LPS-induced macrophages. Cells were incubated with LPS and indicated concentrations of EF for 24 h. (A) Nitrite concentrations in cultured media were determined by Griess reaction. Percentage inhibition of NO production from each treatment is given in relation to nitrite concentration of LPS-stimulated RAW264.7 macrophage cells. Each column shows the mean ± SE of four independent experiments with triplicate samples. ***$p < 0.001$ vs LPS-treated cells. (B) Macrophages were lysed and iNOS as well as β-actin protein levels were determined by Western blot analyses. The immunoblot picture is a representative of 3 separate experiments.

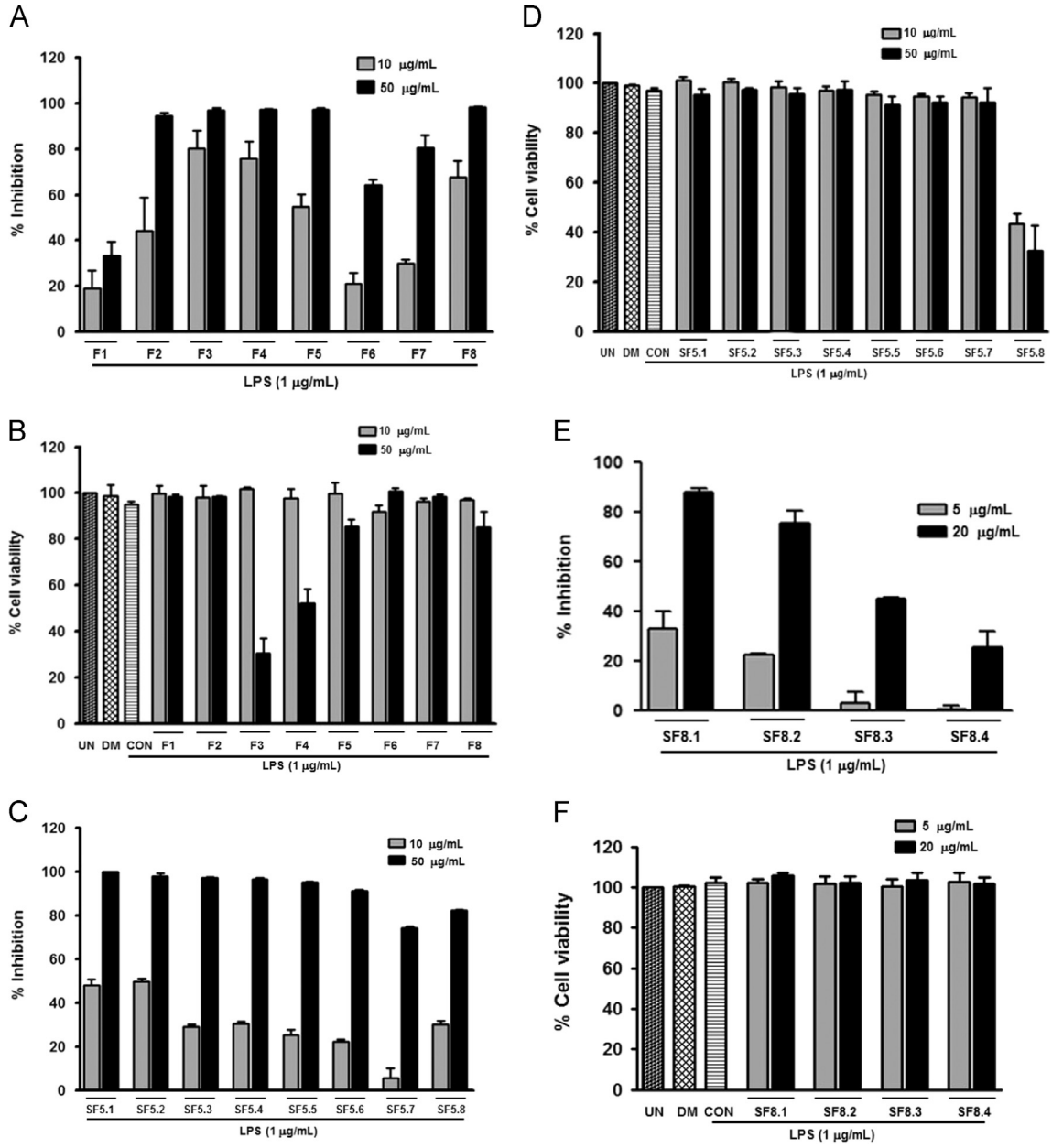

Fig. 4. Effect of fractions from *C. inerme* leaf ethanol extract on nitrite production and cell viability. Cells were co-incubated with the indicated concentrations of LPS and the fractions, (A) F1–F8, (C) SF5.1–SF5.8 and (E) SF8.1–SF8.4. After 24 h, culture media were collected and nitrite concentration was analyzed by Griess reaction. Percentage inhibition of NO production from each treatment is given in relation to nitrite concentration of LPS-stimulated RAW264.7 macrophage cells. Viabilities of cells treated with LPS and the fractions, (B) F1–F8, (D) SF5.1–SF5.8 and (F) SF8.1–SF8.4. Each column shows the mean ± SE of three independent experiments with triplicate samples.

(Fig. 4C and D) and similar thin layer chromatogram (data not shown), were pooled and isolated to afford 3 known flavones, compounds **1**, **2** and **3**. Moreover, compounds **1** and **2** were also obtained from subfractions SF8.1 and 8.2 (the two most NO inhibitory activity without cytotoxicity), respectively (Fig. 4E and F). The structures of the active compounds were elucidated on the basis of their spectroscopic data (HRMS (ESI), ^{1}H- and ^{13}C NMR). The flavone structures were determined by calculating DBE number from their molecular formula (DBE = 11) and the signals of aromatic methine protons and C-3 proton of flavone were also observed in varied chemical shifts ranging from δ_H 6.16 to 8.05 ppm. Finally, the structures were confirmed by comparison of their ^{1}H NMR data with those in the literature. The chemical structures are shown in Fig. 5.

5,7-dihydroxy-2-(4-methoxyphenyl)chromen-4one (4′-methylapigenin or acacetin) (**1**) was obtained as a yellow solid; ^{1}H NMR (DMSO-d_6, 400 MHz): δ3.86 (s, 3H), 6.20 (d, J = 1.7 Hz, 1H), 6.51 (d, J = 1.7 Hz, 1H), 6.88 (s, 1H), 7.11 (d, J = 8.8 Hz, 2H), 8.04 (d, J = 8.8 Hz, 2H), 10.90 (s, br, 1H), 12.92 (s, 1H), ^{13}C NMR (DMSO-d_6, 100 MHz): δ56.0, 94.5, 99.4, 104.0, 104.2, 115.1, 123.3, 128.8, 157.8, 161.9, 162.8, 163.8, 164.7, 182.3. HRMS (ESI): $C_{16}H_{12}O_5$ $[M+Na]^+$, Anal. Cal. 307.0582, Found. 307.0571. These data were consistent with the literature (Ferraro et al., 1987) identifying compound **1** as acacetin.

5,7-dihydroxy-2-(4-hydroxyphenyl)-6-methoxy-4H-chromen-4-one (6-O-methylapigenin or hispidulin) (**2**) was obtained as a yellow solid; ^{1}H NMR (DMSO-*d6*, 400 MHz): δ 3.74 (s, 3H), 6.59 (s, 1H), 6.78 (s, 1H), 6.92 (d, J = 8.5 Hz, 2H), 7.92 (d, J = 8.5 Hz, 2H), 10.42 (s, br, 1H), 13.08 (s, 1H), ^{13}C NMR (DMSO-d_6, 100 MHz): δ60.4, 94.7, 102.8, 104.5, 116.4, 121.7, 128.9, 131.8, 152.9, 153.2, 157.8, 161.6, 164.3, 182.6. HRMS (ESI): $C_{16}H_{12}O_6$ $[M+Na]^+$, Anal. Cal. 323.0532, Found. 323.0534. Compared with the literature (Hazekamp et al., 2001), compound **2** was identified as hispidulin.

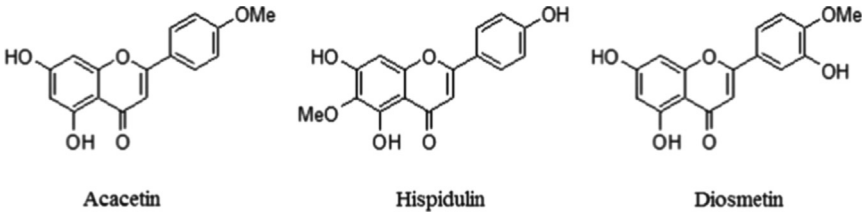

Fig. 5. Chemical structure of acacetin (**1**), hispidulin (**2**) and diosmetin (**3**).

5,7-dihydroxy-2-(3-hydroxy-4-methoxyphenyl)chromen-4-one (diosmetin) (**3**) was obtained as a yellow solid; ^{1}H NMR (DMSO-d_6, 400 MHz): δ3.86 (s, 3H), 6.16 (s, 1H), 6.43 (s, 1H), 6.74 (s, 1H), 7.09 (d, J=8.5 Hz, 1H), 7.42 (d, J=1.9 Hz, 1H), 7.54 (dd, J=1.9, 8.5 Hz, 1H), 9.55 (brs, 1H), 12.92 (s, 1H),. HRMS (ESI): $C_{16}H_{12}O_6$ $[M+Na]^+$, Anal. Cal. 323.0532, Found. 323.0534. Compound **3** was identified as diosmetin from the spectroscopic data (Ninomiya et al., 2013).

C. inerme plant is reported to contain a variety of phytochemicals (Shrivastava and Patel, 2007b; Parveen et al., 2010; Shahabuddin et al., 2013). The isolation of acacetin from *C. inerme* in this study is in agreement with the earlier reports by Shrivastava and Patel (2007b). The other two flavones, hispidulin and diosmetin, isolated in this study are also known compounds, however, to the best of our knowledge; this is the first report of their isolation from *C. inerme* leaves. Hispidulin has been isolated from some species of *Clerodendrum* including *Clerodendrum indicum*, *Clerodendrum petasites* and *Clerodendrum infortunatum* (Hazekamp et al., 2001; Shrivastava and Patel, 2007b). The three isolated flavones were examined for NO inhibitory activity by treating macrophages with flavones and LPS. All three flavones showed a dose-dependent inhibition of NO production and no significant cytotoxicity to concentrations of 100 μM (Fig. 6). IC_{50} values of acacetin, hispidulin and diosmetin were 43.5 ± 6.4, 43.7 ± 4.0 and 57.1 ± 4.0 μM, respectively. Aminoguanidine also inhibited NO production in a dose-dependent manner with an IC_{50} value of 54.1 ± 4.9 μM (Fig. 6). The inhibitory activity against NO of acacetin and hispidulin was higher than that of aminoguanidine. Nevertheless, in accordance with many reports showing anti-inflammatory effect of flavones (Matsuda et al., 2003; Pan et al., 2006; Nam et al., 2013), acacetin, hispidulin and diosmetin were found to exert anti-inflammatory activity via inhibition of NO production in LPS-stimulated macrophages. These results indicated that in *C. inerme* leaves, three flavones may contribute to anti-inflammatory activity. Acacetin inhibited NO and PGE_2 production through suppression of LPS-induced iNOS and COX-2 expression in macrophages (Pan et al., 2006). Matsuda et al. (2003) found diosmetin down-regulated NO production and iNOS protein expression in peritoneal macrophages. Hispidulin has been shown to act as bronchiodilator in guinea-pig tracheal smooth muscle exposed to histamine (Hazekamp et al., 2001). Also, hispidulin showed anti-inflammatory activity by inhibiting 5-lipoxygenase pathway in porcine leukocyte (Moongkarndi et al., 1991) and inhibiting croton oil-induced mouse ear edema (Cottiglia et al., 2005). Recently, this compound has been reported to inhibit LPS/IFN-γ-induced NO production in RAW 264.7 macrophages (Alza et al., 2014). However, the molecular mechanism underlying the anti-inflammatory activity of hispidulin remains unclear. Besides NO, PGE_2 was found to be involved in inflammatory disorders (Kang et al., 2007). In the present study, hispidulin in LPS-induced macrophages caused a dose-dependent reduction in COX-2-catalyzed PGE_2 production with an IC_{50} value of 12.4 ± 4.2 μM (Fig. 7A) compared to the positive control indomethacin. Indomethacin is a COX inhibitor (Utar et al., 2011) with a 99.9 ± 0.07% inhibition of PGE_2 at 10 μM.

The effect of hisidulin on iNOS and COX-2 expressions was determined since both proteins are regulated primarily at the transcriptional level (Kleinert et al., 2003; Kang et al., 2007). iNOS and COX-2 were undetectable in unstimulated cells (control cells) while

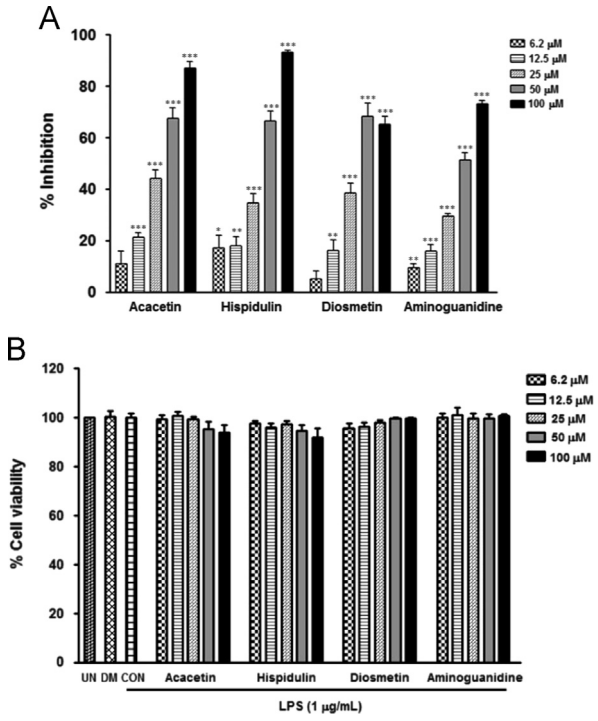

Fig. 6. Inhibitory effects on NO production of isolated flavones. Cells were incubated with LPS and various concentrations of tested compounds for 24 h. (A) Nitrite inhibition in relation to concentration, 6.2–100 μM, of each of the four flavones. The percentage inhibition of NO production of each treatment was determined in comparison to LPS-stimulated RAW264.7 macrophage cells. (B) Viabilities of cells treated with LPS and each flavone. Each column shows the mean ± SE of three independent experiments with triplicate samples. *$p < 0.05$, **$p < 0.01$, ***$p < 0.001$ vs LPS-treated cells, respectively.

LPS treatment dramatically increased the expression of both and hispidulin suppressed the protein levels of both in a concentration-dependent manner (Fig. 7B). In accordance with protein level, hispidulin markedly inhibited the expression of iNOS and COX-2 mRNA (Fig. 8A and B). In accord, Yu et al. (2013) demonstrated that hispidulin down-regulated COX-2 expression in AGS human gastric adenocarcinoma cell line. The high inhibitory effect of hispidulin on PGE_2 production relative to COX-2 protein expression is noteworthy but may indicate the presence of another mechanism (Fig. 7).

It is well-known that the NF-κB pathway is involved in modulating LPS-induced iNOS and COX-2 expression in macrophages (Chun et al., 2012). Ubiquitous NF-κB in mammalian cells is composed of two major subunits: p65 and p50. In un-stimulated macrophages, NF-κB is present in the cytoplasm and is bound by the inhibitory protein, IκB. Upon stimulation with LPS, IκB is phosphorylated and degraded leading to the translocation of NF-κB to the nucleus where it binds with the promoters of target genes including iNOS and COX-2, ultimately regulating gene expression (Nishikori, 2005). Since we found hispidulin inhibited the expression of iNOS and COX-2 mRNA and protein suggesting it

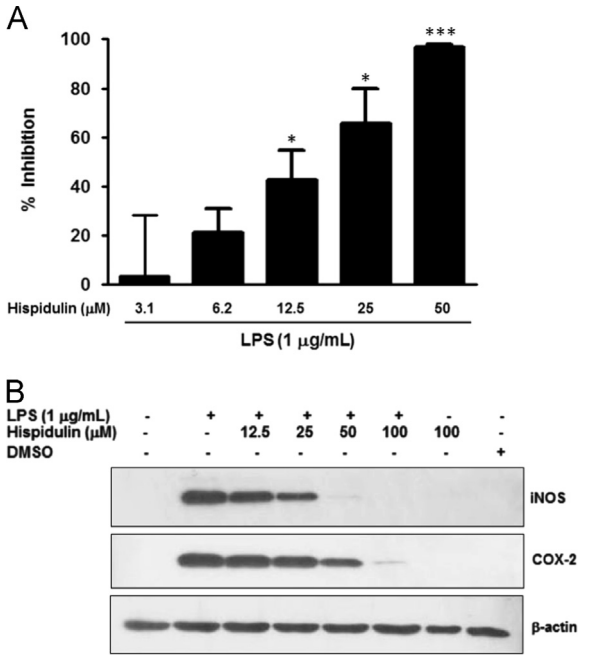

Fig. 7. Effect of hispidulin on PGE_2 production and iNOS as well as COX-2 expression. Macrophages were incubated with LPS and indicated concentrations of hispidulin for 24 h. (A) PGE_2 concentration in cultured media was determined with a PGE_2 competitive enzyme immunoassay kit. Percentage inhibition of PGE_2 production following each treatment was determined in comparison to LPS-stimulated RAW264.7 macrophage cells. Each column shows the mean ± SE of three independent experiments with triplicate samples. $^{*}p < 0.05$, $^{***}p < 0.001$ vs LPS-treated cells, respectively. (B) iNOS, COX-2 and β-actin protein levels were determined by Western blot analyses. The immunoblot picture is a representative of 3 separate experiments.

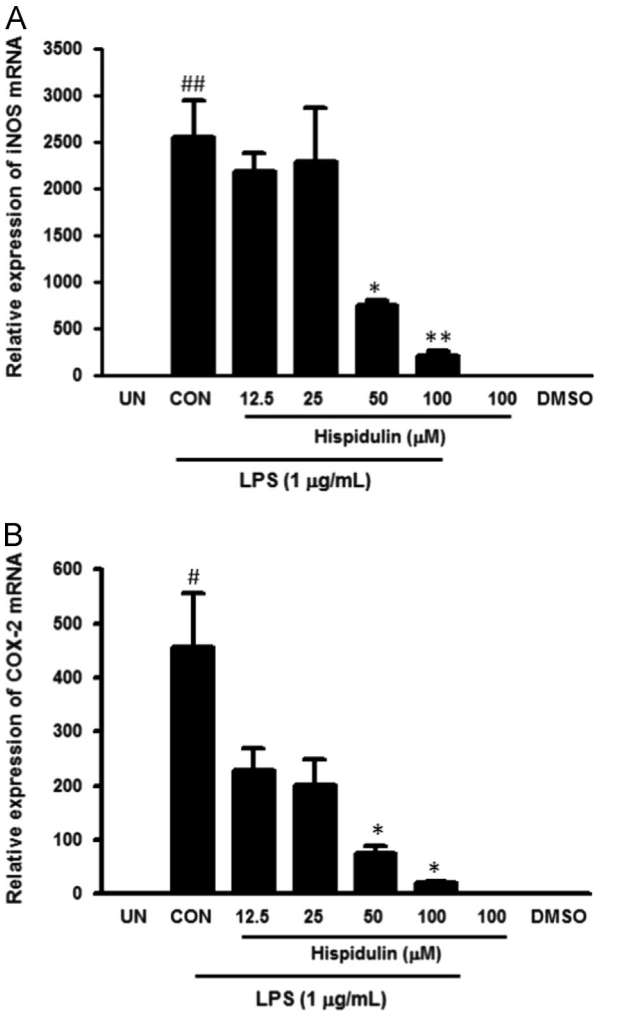

Fig. 8. Inhibitory effects of hispidulin on iNOS and COX-2 mRNA expressions in LPS-induced RAW 264.7 cells. (A) Cells were stimulated with LPS and indicated concentrations of hispidulin for 9 h. Cells were lyzed, and total RNA was isolated. iNOS and COX-2 mRNA levels were determined by real-time RT-PCR. Each column shows the mean ± SE of three independent experiments with triplicate samples. $p < 0.05$, vs unstimulated macrophage cells. $^{*}p < 0.05$, $^{**}p < 0.01$ vs LPS alone. UN = unstimulated control cells, CON = LPS-stimulated cells and DMSO = 0.2% (v/v) DMSO-treated cells.

may regulate this upstream signaling pathway. We next determined if hispidulin affects the nuclear translocation of NF-κB p65 subunit. LPS increased the level of NF-κB p65 protein subunit in nuclear protein (Fig. 9A). Hispidulin at concentrations of 12.5–100 μM failed to decrease quantities of NF-κB p65 subunit in the nucleus of LPS-stimulated cells relative to cells treated with only LPS. Interestingly, hispidulin significantly inhibited the DNA binding activity of activated NF-κB (Fig. 9B) indicating it down-regulated iNOS and COX-2 expression, at least in part, by suppression of NF-κB DNA binding activity but it did not affect the nuclear translocation of NF-κB p65 subunit. This was in agreement with the observation that nobiletin, an isolated compound from *Citrus sunki*, inhibited NO and PGE_2 production via reduction of NF-κB DNA binding activity without direct interaction with NF-κB (Choi et al., 2007). However, nobiletin failed to inhibit either IκB phosphorylation or translocation of NF-κB p65 subunit to nucleus in LPS-stimulated RAW 264.7 macrophages. Similarly, andrographolides have been found to interfere directly with the binding of NF-κB and DNA but do not affect nuclear translocation of p65 subunit and degradation of IκBα in endothelial and HL-60/neutrophils (Xia et al., 2004; Hidalgo et al., 2005). This suggests that either hispidulin itself or a metabolite may inhibit the interaction between NF-κB and DNA leading to suppression of iNOS and COX-2 expression. However further studies are required to clarify the exact mechanism by which hispidulin inhibited NF-κB DNA binding activity in macrophages treated with LPS.

Multiple lines of evidence indicate MAPKs signaling pathways play a role in regulation of iNOS and COX-2 expression (Chen et al., 1999; Chun et al., 2012; Buapool et al., 2013). MAPKs activation requires the phosphorylation of threonine and tyrosine residues (Chun et al., 2012). To determine whether MAPKs activation involved in the suppression of iNOS and COX-2 expression by hispidulin, the level of MAPKs phosphorylation was determined by Western blot analysis. LPS treatment caused phosphorylation of all three MAPKs while hispidulin reduced the phosphor JNK in a dose-dependent manner but not ERK1/2 and p38 (Fig. 10). Thus, this result suggested that the inhibition of JNK phosphorylation by hispidulin seems to be involved in suppression of LPS-induced iNOS and COX-2 expression.

In conclusion, three flavones, in part, responsible for anti-inflammatory effects of *C. inerme* leaves were isolated by bioassay-guided isolation. Among the three compounds, hispidulin is a potent inhibitor of NO and PGE_2 production by inhibiting NF-κB DNA-binding activity and JNK signaling pathway, subsequently suppressing iNOS and COX-2 expression. This is the explanation of the molecular mechanism underlying anti-inflammatory activity of hispidulin. Our data provide scientific evidence to clarify the therapeutic effects of *C. inerme* leaves in traditional medicine and also suggest that hispidulin is a potential candidate for treatment of inflammatory-related diseases.

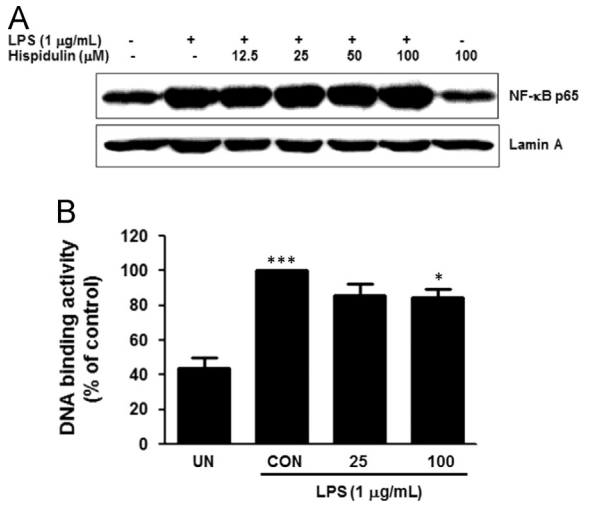

Fig. 9. Effect of hispidulin on NF-κB p65 subunit nuclear translocation in LPS-stimulated macrophages. Cells were pretreated with indicated concentrations of hispidulin for 30 min followed by LPS for 1 h. Nuclear proteins were extracted, then protein levels of NF-κB p65 subunit and lamina A were analyzed by Western blot analyses (A). The gel picture shown is a representative of 5 separated experiments. (B) NF-κB binding activity of nuclear protein from RAW 264.7 macrophages using NF-κB p65 ELISA-based transcription factor assay kit as described in method. The percentage of NF-κB binding activity of each treatment was determined in comparison to LPS-stimulated RAW264.7 macrophage cells (CON). Each column shows the mean ± SE of four independent experiments. $p < 0.001$ vs unstimulated macrophage cells (UN). *$p < 0.05$ vs LPS alone (CON).

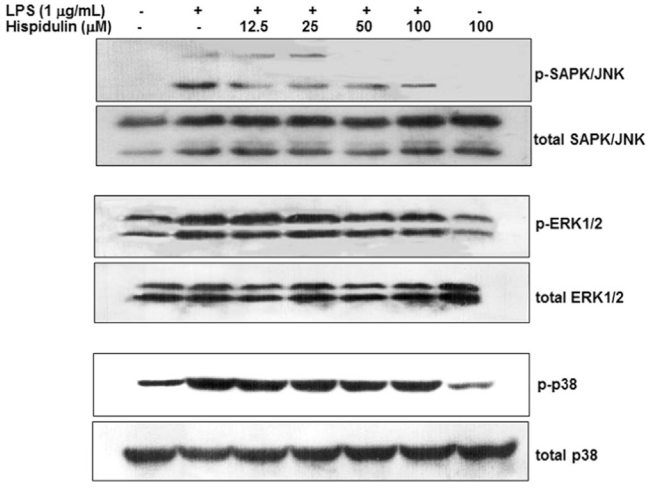

Fig. 10. Effect of hispidulin on LPS-induced phosphorylation of MAPKs in macrophages. Cells were incubated with LPS for 30 min after exposure to indicated concentrations of hispidulin for 30 min. Total MAPKs and phosphor-MAPKs were analyzed by Western blot analyses. The immuno blot picture shown is a representative of 3 separated experiments.

Conflict of interests

The authors have no conflict of interest to declare.

Acknowledgments

The work was financially supported by Burapha University (35/2554 and 12/2555) and the Centre of Excellence for Innovation in Chemistry (PERCH-CIC), Commission on Higher Education, Ministry of Education, Thailand. Authors wish to thank Professor Frederick W.H. Beamish, Faculty of Science, Burapha University, for his comments and English correction. We are thankful to Ms. Supatra Purintaraworakul and Ms. Sarinporn Udompong for valuable technical assistance.

References

Alderton, W.K., Cooper, C.E., Knowles, R.G., 2001. Nitric oxide synthases: structure, function and inhibition. Biochemical Journal 357, 593–615.

Alza, N.P., Pferschy-Wenzig, E.M., Ortmann, S., Kretschmer, N., Kunert, O., Rechberger, G.N., Bauer, R., Murray, A.P., 2014. Inhibition of NO production by *Grindelia argentina* and isolation of three new cytotoxic saponins. Chemical Biodiversity 11, 311–322.

Buapool, D., Mongkol, N., Chantimal, J., Roytrakul, S., Srisook, E., Srisook, K., 2013. Molecular mechanism of anti-inflammatory activity of *Pluchea indica* leaves in macrophages RAW 264.7 and its action in animal models of inflammation. Journal of Ethnopharmacology 4, 495–504.

Chethana, G.S., Hari, V.K.R., Gopinath, S.M., 2013. Review on *Clerodendrum inerme*. Journal of Pharmaceutical and Scientific Innovation 2, 38–40.

Chen, B.C., Chen, Y.H., Lin, W.W., 1999. Invlovement of p38 mitogen-activated protein kinase in lipopolysaccharide-induced iNOS and COX-2 expression in J774 macrophage. Immunology 97, 124–129.

Choi, S.Y., Hwang, J.H., Ko, H.C., Park, J.G., Kim, S.J., 2007. Nobiletin from citrus fruit peel inhibits the DNA-binding activity of NF-κB and ROS production in LPS-activated RAW 264.7 cells. Journal of Ethnopharmacology 113, 149–155.

Chun, J., Choi, R.J., Khan, S., Lee, D.S., Kim, Y.C., Nam, Y.J., Lee, D.U., Kim, Y.S., 2012. Alantolactone suppresses inducible nitric oxide synthase and cyclooxygenase-2 expression in LPS-activated RAW 264.7 cells. International Immunopharmacology 14, 375–383.

Cottiglia, F., Casu, L., Bonsignore, L., Casu, M., Floris, C., Sosa, S., Altinier, G., Della Logia, R., 2005. Topical anti-inflammatory activity of flavonoids and a new xanthone from *Santolina insularis*. Zeitschrift fur Naturforschung C: Journal of Biosciences 60, 63–66.

Ferraro, G., Martino, V., Borrajo, G., Coussio, J.D., 1987. 5,7,3′,4′-Tetrahydroxy-6-methoxyflavanone from *Eupatorium subhastatum*. Phytochemistry 26, 3092–3093.

Giulietti, A., Overbergh, L., Valckx, D., Decallonne, B., Bouillon, R., Mathieu, C., 2001. An Overview of real-time quantitative PCR: applications to quantify cytokine gene expression. Methods 25, 386–401.

Gopal, N., Sengottuvelu, S., 2008. Hepatoprotective activity of *Clerodendrum inerme* against CCl4 induced hepatic injury in rats. Fitoterapia 79, 24–26.

Gurudeeban, S., Satyavani, K., Ramanathan, T., Umamaheswari, G., Shanmugapriya, R., 2010. Antioxidant and radical scavenging effect of *Clerodendrum inerme* (L.). World Journal of Fish and Marine Sciences 2, 66–69.

Hazekamp, A., Verpoorte, R., Panthong, A., 2001. Isolation of a bronchodilator flavonoids from Thai medicinal plant *Cleodendrum petasites*. Journal of Ethnopharmacology 78, 45–49.

Hidalgo, M.A., Romero, A., Figueroa, J., Cortes, P., Concha, I.I., Hancke, J.L., Burgos, R.A., 2005. Andrographolide interferes with binding of nuclear factor-κB to DNA in HL-6-derived neutrophilic cells. British Journal of Pharmacology 144, 680–686.

Kang, Y.J., Mbonye, U.R., DeLong, C.J., Wada, M., Smith, W.L., 2007. Regulation of intracellular cyclooxygenase levels by gene transcription and protein degradation. Progress in Lipid Research 46, 108–125.

Khanam, D., Deb, D., Dev, S., Shahriar, M., Das, A.K., Kawsar, M.H., 2014. Analgesic and anti-inflammatory activities of ethanolic extract of *Clerodendrum inerme* (L.) Gaertn. Bangladesh Pharmaceutical Journal 17, 62–66.

Kalavathi, R., Sagayagiri, R., 2014. Phytochemical screening and anti-inflammatory activity of *Clerodendrum inerme* L. (Gaertn). International Journal of Research in Plant Science 4, 92–95.

Kleinert, H., Schwarz, P.M., Förstermann, U., 2003. Regulation of the expression of inducible nitric oxide synthase. Biological Chemistry 384, 1343–1364.

Kumar, V., Abbas, A.K., Fausto, N., Mitchell, R.N., 2007. Robbins Basic Pathology, eight ed. Elsevier Saunders, United States of America.

Matsuda, H., Morikawa, T., Ando, S., Toguchida, I., Yoshikawa, M., 2003. Structural requirements of flavonoids for nitric oxide production inhibitory activity and mechanism of action. Bioorganic and Medicinal Chemistry 11, 1995–2000.

Moongkarndi, P., Bunyapraphatsara, N., Srisukh, V., Wagne, H., 1991. The inhibitory activity in 5-lipoxygenase pathway of hispidulin from Millngtonia hortensis Linn. Journal of Science Society of Thailand 17, 51–56.

Nam, Y., Choi, M., Hwang, H., Lee, M.G., Kwon, B.M., Lee, W.H., Suk, K., 2013. Natural flavone jaceosidin is a neuroinflammation inhibitor. Phytotherapy Research 27, 404–411.

Ninomiya, M., Nishida, K., Tanaka, K., Watanabe, K., Koketsu, M., 2013. Structure-activity relationship studies of 5, 7-dihydroxyflavones as naturally occurring inhibitors of cell proliferation in human leukemia HL-60 cells. Journal of Nature Medicine 67, 460–467.

Nishikori, M., 2005. Classical and alternative NF-κB activation pathways and their roles in lymphoid malignancies. Journal of Clinical and Experimental Hematopathology 45, 15–24.

Office of Mangrove Resources Conservation, Department of Marine and Coastal Resources, Ministry of Natural Resources and Environment, 2009. Plants in the Mangrove forest of Thailand. Printing house of the Agricultural Co-operative Federation of Thailand Limited, Nonthaburi, (In Thai).

Pan, M.H., Lai, C.S., Wang, Y.J., Ho, C.T., 2006. Acacetin suppressed LPS-induced upexpression of iNOS and COX-2 in murine macrophages and TPA-induced tumor promotion in mice. Biochemical Pharmacology 72, 1293–1303.

Parveen, M., Khanam, Z., Ali, M., Rahman, S.Z., 2010. A novel lupene-type triterpenic glucoside from the leaves of *Clerodendrum inerme*. Natural Product Research 24, 167–176.

Sangeetha, M., Kousalya, K., Lavanya, R., Sowmya, C., Chamundeewari, D., Reddy, C. U.M., 2011. In vitro anti-inflammatory and anti-arthritic activity of leaves of *Clerodendrum inerme*. Reserch Journal of Pharmaceutical, Biological and Chemical Sciences 2, 822–827.

Shahabuddin, S.K., Munikishore, R., Trimurtulu, G., Gunasekar, D., Devillee, A., Bodo, B., 2013. Two new chalcones from the flowers of *Clerodendrum inerme*. Natural Product Communications 8, 459–460.

Shrivastava, N., Patel, T., 2007a. Clerodendrum and healthcare: an overview. Medicinal and Aromatic Plant Science and Biotechnology 1, 142–150.

Shrivastava, N., Patel, T., 2007b. Clerodendrum and healthcare: an overview-part II phytochemistry and biotechnology. Medicinal and Aromatic Plant Science and Biotechnology 1, 209–223.

Utar, Z., Majid, M.I., Adenan, M., Jamil, M.F., Lan, T.M., 2011. Mitragynine inhibits the COX-2 mRNA expression and prostaglandin E_2 production induced by lipopolysaccharide in RAW264.7 macrophage cells. Journal of Ethnopharmacology 136, 75–82.

Xia, Y.F., Ye, B.Q., Li, Y.D., Wang, J.G., He, X.J., Lin, X., Yao, X., Ma, D., Slungaard, A., Hebbel, R.P., Key, N.S., Geng, J.G., 2004. Andrographolide attenuates inflammation by inhibition of NF-κ B activation through covalent modification of reduced cysteine 62 of p50. Journal of Immunology 173, 4207–4217.

Yang, Y., Yu, T., Lee, Y.G., Yang, W.S., Oh, J., Jeong, D., Lee, S., Kim, T.W., Park, Y.C., Sung, G.H., Cho, J.Y., 2013. Methanol extract of *Hopea odorata* suppresses inflammatory responses via the direct inhibition of multiple kinases. Journal of Ethnopharmacology 145, 598–607.

Yankanchi, S.R., Koli, S.A., 2010. Anti-inflammatory and analgesic activity of mature leaves methanol extract of *Clerodendrum inerme* L.(Gaertn). Journal of Pharmaceutical Sciences and Research 2, 782–785.

Yu, C.Y., Su, K.Y., Lee, P.L., Jhan, J.Y., Tsao, P.H., Chan, D.C., Chen, Y.L., 2013. Potential therapeutic role of hispidulin in gastric cancer through induction of apoptosis via NAG-1 signaling. Evidence Based Complementary and Alternative Medicine 2013, 12 518301.